Journal of Nuclear Materials 394 (2009) 109–113

Contents lists available at ScienceDirect

Journal of Nuclear Materials

journal homepage: www.elsevier.com/locate/jnucmat

Absorbed impact energy and mode of fracture: A statistical description of the micro-structural dispersion

V. Pontikis *, D. Gorse

Commissariat à l'Energie Atomique, IRAMIS, Laboratoire des Solides Irradiés, CNRS UMR 7642, Ecole Polytechnique, 91191 Gif sur Yvette Cedex, France

ARTICLE INFO

Article history:
Received 24 April 2009
Accepted 21 August 2009

PACS:
46.50.+a
46.80.tj
62.25.mn
81.70.Bt

ABSTRACT

A statistical model is proposed to account for the influence of the dispersion of the microstructure on the ductile-to-brittle transition in body centered cubic (bcc) metals and their alloys. In this model, the dispersion of the microstructure is expressed via a normal distribution of transition temperatures whereas a simple relation exists between the values of absorbed, lower and upper shelf energies, the ductile area fraction and the distribution parameters. It is shown that via an appropriate renormalization of energies and temperatures, experimental data for different materials and ageing conditions align all together on a master curve, guaranteeing thereby the effectiveness of the proposed statistical description.

© 2009 Elsevier B.V. All rights reserved.

1. Introduction

It is established that the mechanical response of bcc metals and of their alloys (e.g. ferritic steels) to an external stress transforms from brittle to ductile on increasing the temperature [1–3]. This behavior is related to the increase with temperature of the fracture toughness of the material and attests for the evolving competition between underlying mechanisms of failure. The crossover between brittle and plastic failure modes is often referred to as the "ductile-to-brittle transition", though it does not originate from a thermodynamic phase transformation.

In the popular Charpy test [1], the ductile-to-brittle transition temperature, T_{DBT}, is determined by the absorbed energy reaching an arbitrarily fixed threshold value for the sample under test. When testing several, nominally identical samples, it is commonly observed that in the transition region, the absorbed energy values are largely scattered [4] whereas different plateau values, brittle (lower shelf) and ductile (upper shelf), are obtained from dynamic or static mechanical tests [5]. Moreover, this dispersion is characteristic of all the kinds of experimental determinations of the fracture toughness whereas for a given material T_{DBT} values are sample-size dependent.

Associated to the measurement of the absorbed energy, the examination of fracture surfaces provides a qualitative description of the failure mode subsequently labeled as intergranular brittle, transgranular brittle, ductile or mixed. In the transition region, a mixed mode is always observed i.e. fracture surfaces consist in a mixture of areas with brittle or ductile features, suggesting the increase of the absorbed energy with the temperature be related to an increasing fraction of the material undergoing ductile failure. Most of the published observations of fracture surfaces are qualitative, aiming at the identification of the dominant fracture mode. In recent works however, the approach has been extended by means of quantitative fractography showing that in fracture surfaces the distribution of ductile and brittle areas is highly heterogeneous and that in static tests the ductile fraction is higher than in dynamic tests [5]. Finally, it has been remarked that in brittle fracture, plastic deformation can be present at a microscopic scale without any macroscopic evidence of ductility since dislocations are needed for initiating cleavage [5].

Macroscopic modeling of the impact test has been devoted to the derivation of reasonable forms for fitting the experimental results and for obtaining estimates of models parameters and of the associated standard errors [4,6,7]. However, no generally accepted distribution function has been proposed accounting for the variability in the proportions of brittle and ductile fracture stemming from the dispersion in the microstructures of the samples.

In this work, a physically motivated statistical distribution function is proposed for describing the ductile fraction in an impact test specimen as a function of the temperature. This distribution accounts for the variability of the ductile fraction, stemming from the dispersion of the specimen microstructure. In the following paragraphs, the model is introduced and its principal implications are derived. The validation of the model is then made through a comparison with experimental data for steels [8,13–17] and refractory metals [9–11] from the literature. Finally, the results are

* Corresponding author. Tel.: +33 1 6908 2904.
E-mail addresses: Vassilis.Pontikis@cea.fr, Vassilis.Pontikis@wanadoo.fr (V. Pontikis).

0022-3115/$ - see front matter © 2009 Elsevier B.V. All rights reserved.
doi:10.1016/j.jnucmat.2009.08.015

discussed and reasons in favor of further developing quantitative fractography are given.

2. The model

Due to their microstructures, real materials are heterogeneous even for states close to the thermodynamic equilibrium. It is therefore expected that conditions under which a fracture can nucleate and propagate are position dependent. Let us denote T_0, the ductile-to-brittle transition temperature for the average material taken as the reference and dn, the number of regions (grains) having at the temperature T, a ductile-to-brittle transition temperature in the range $[T, T + dT]$. It is then reasonable to assume that, dn, is normally distributed:

$$dn = \rho(T)dT = A\exp\left[\frac{(T-T_0)^2}{2\sigma^2}\right]dT \tag{1}$$

where, A, is a normalization constant and σ^2, the variance of the normal distribution expressing the micro-structural dispersion. If, N, is the total number of such regions, A, is determined by integrating (1):

$$\begin{cases} N = \int_0^{T_m} A\exp\left[\frac{(T-T_0)^2}{2\sigma^2}\right]dT \\ A = \sqrt{\frac{2}{\pi}}\frac{N}{\sigma B} \\ B = \mathrm{erf}\left(\frac{T_m-T_0}{\sigma\sqrt{2}}\right) + \mathrm{erf}\left(\frac{T_0}{\sigma\sqrt{2}}\right) \end{cases} \tag{2}$$

where, T_m, is the melting point temperature and "erf" denotes the error function. The fraction, $f(T)$, of micro-structural regions (grains) having undergone the transition at any temperature, T, is then given by

$$f(T) = \frac{n(T_{DBT} \leqslant T)}{N} = \frac{1}{N}\int_0^T \rho(T)\,dT = \frac{\mathrm{erf}\left(\frac{T-T_0}{\sigma\sqrt{2}}\right) + \mathrm{erf}\left(\frac{T_0}{\sigma\sqrt{2}}\right)}{\mathrm{erf}\left(\frac{T_m-T_0}{\sigma\sqrt{2}}\right) + \mathrm{erf}\left(\frac{T_0}{\sigma\sqrt{2}}\right)} \tag{3}$$

Assuming that the controlling factor determining the level of the absorbed impact energy, $E(T)$, is the proportion of the material likely to fracture in the ductile mode, the following linear relation, already used by others, holds [6]:

$$E(T) = E_{LS} + (E_{US} - E_{LS})f(T) \tag{4}$$

where, E_{LS} and E_{US}, represent respectively the lower and upper shelf energies. Whenever $T_m \gg T_0$ and $T_0 \gg \sigma$, instead of Eq. (4) the following approximated expression can be used with excellent accuracy:

$$E(T) \approx E_{LS} + \frac{1}{2}(E_{US} - E_{LS})\left[1 + \mathrm{erf}\left(\frac{T-T_0}{\sigma\sqrt{2}}\right)\right] \tag{5}$$

Provided the assumptions leading to Eqs. (3) and (4) are realistic, the proposed model predicts the existence of a master curve, $E^* = \mathrm{erf}(T^*)$, obtained by rescaling the coordinates. This curve is expected fitting experimental data whatever the materials studied and the ageing mechanisms controlling the ductile-to-brittle transition temperature e.g. thermal, mechanical or irradiation. The rescaled coordinates, E^* and T^*, are given by

$$\begin{cases} E^* = \left(\frac{E(T)-E_{LS}}{E_{US}-E_{LS}}\right)B - \mathrm{erf}\left(\frac{T_0}{\sigma\sqrt{2}}\right) \\ T^* = \frac{T-T_0}{\sigma\sqrt{2}} \end{cases} \tag{6}$$

Similarly, the rescaled ductile fraction, F^*, is given by

$$F^*(T^*) = f(T^*)B - \mathrm{erf}\left(\frac{T_0}{\sigma\sqrt{2}}\right) \approx 2f(T^*) - 1 \tag{7}$$

Table 1
Model parameters, E_{LS}, E_{US}, s and T_0, adjusted to experimental data from the literature for different materials and ageing conditions. E_{LS} and E_{US} are the lower and upper shelf energies whereas T_0 represents the transition temperature and s the standard deviation.

Material	T_0 (K)	σ (K)	E_{LS} (mJ/m^2)	E_{US} (mJ/m^2)	Reference
Steel A508C13	249	39	0.12	22.58	[8]
Steel A508C13 neutron irradiated[a]	352	37.5	0.72	16.72	[8]
Nb	249	10.15	0.97	26.06	[9]
V	322	0.1	0.109	1.04	[10]
W	1070	101.7	0.037	1.11	[11]

[a] Irradiation conditions: $T = 563$ K, dose: 3.2×10^{19} neutrons/cm^2 ($E > 1$ MeV), dose rate: 10^{13} neutrons/cm^2/s.

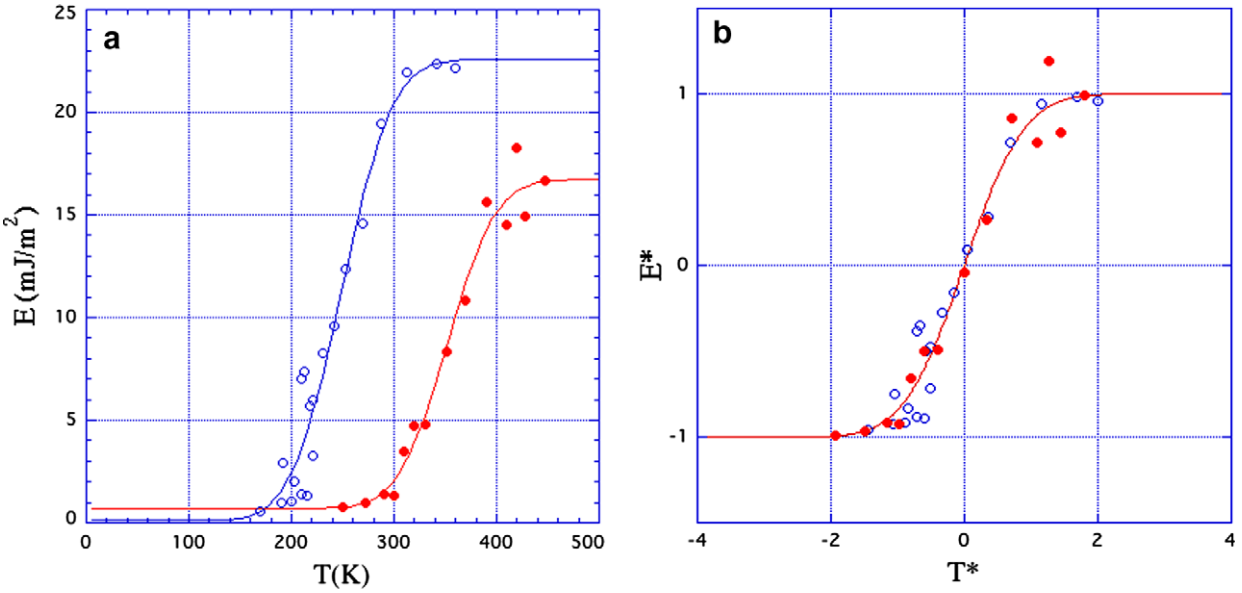

Fig. 1. Absorbed impact energy for steel 16MND5 (SA508C13) plotted as a function of the temperature: (a) experimental data before (open circles) and after irradiation (full circles) from Ref. [8]. Full lines are best fits of Eq. (4) to the experimental data; (b) master curve (full line) and the above experimental data after rescaling (Eq. (6)). Values of the fitting parameters are given in Table 1.

In this model, the macroscopic transition temperature, T_0, corresponds to the inflexion point of the error function (Eqs. (3)–(5)) defined as the weighted average of ductile-to-brittle transition temperatures of the regions composing the sample. T_0 can be determined by fitting Eq. (4) on the absorbed impact energy data or, equivalently, Eq. (3) on the ductile fraction data obtained from quantitative fractography.

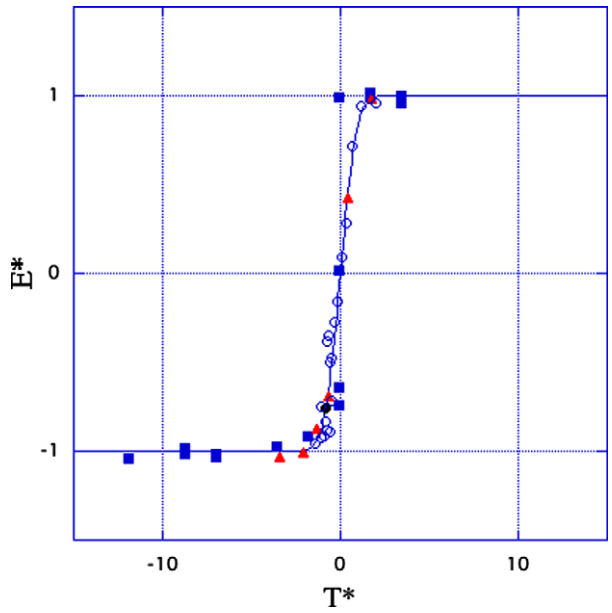

Fig. 2. Absorbed impact energy plotted as a function of the temperature. Master curve (full line, Eq. (6)) and experimental data for steel 16MND5 (SA508C13) (open circles, [8]), Nb (full squares, [9]), V (full circles, [10]) and W (full triangles, [11]).Values of the fitting parameters are given in Table 1.

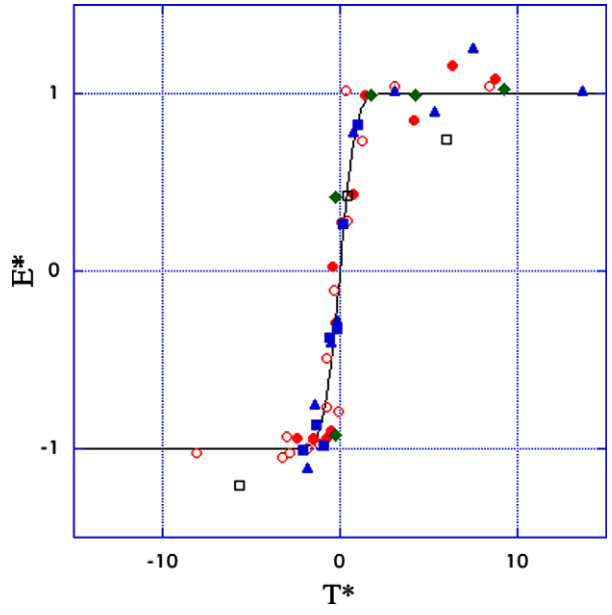

Fig. 3. Absorbed impact energy plotted as a function of the temperature. Master curve (full line, Eq. (6)) and experimental data for steel F82H. Full and open circles: CVN and MCVN samples [15], full diamonds: MCVN samples [16], full triangles: small punch test samples [14], full and open squares: CVN samples with impact direction respectively parallel or normal to the rolling direction [13].Values of the fitting parameters are given in Table 2.

3. Comparison with experiments

The relevance of the model is here tested by seeking its ability to fit experimental data for steels and refractory metals extracted from the literature. Fig. 1a displays data of Charpy V-notched specimens (referred hereafter to as CVN) for steel 16MND5 (close to grade ASME SA508C13) before and after irradiation [8], together with the best fits of Eq. (4) to the data. The fit parameters are listed in Table 1. The overall quality of the fit is satisfactory whereas the extracted value of the transition temperature shift after irradiation, $\delta T_0 \approx 103$ K, is close to the value reported by the authors, $\delta T_{DBT} = 111$ K [8]. By rescaling the energy and temperature (Eq. (6)) the data align on the master curve displayed in Fig. 1b.

In Fig. 2, the master curve is drawn together with the above experimental data for steel 16MND5 [8] and data for niobium [9], vanadium [10] and tungsten [11]. The fit parameters are listed in Table 1. Irrespective to the considered material all the rescaled experimental data align on the master curve with little residual scatter. Both Figs. 1b and 2, indicate that in these reference and irradiated materials the mechanisms of plastic energy absorption

Table 2
Model parameters fitted to experimental data for steel F82H with different sample dimensions CVN, MCVN and small disks adapted to Charpy and small punch tests. T_{DBT} is the transition temperature value reported in the referenced works.

Sample	T_0 (K)	σ (K)	E_{LS} (mJ/m^2)	E_{US} (mJ/m^2)	T_{DBT} (K)	Reference
Small punch	112	9.5	0.006	0.023	109	[14]
MCVN	182	9.2	0.033	0.93	173 ± 5	[15]
MCVN	213	1.5	0.0225	0.906	214	[16]
MCVN	176	0.1	0.05	0.98	–	[17]
CVN	220	5.8	0	30.0	223 ± 10	[15]
CVN	228	18.5	0.425	32.5	234	[13][a]
CVN	218	0.6	0.424	26.1	225	[13][b]

[a] Impact direction: normal.
[b] Impact direction: parallel to the rolling direction.

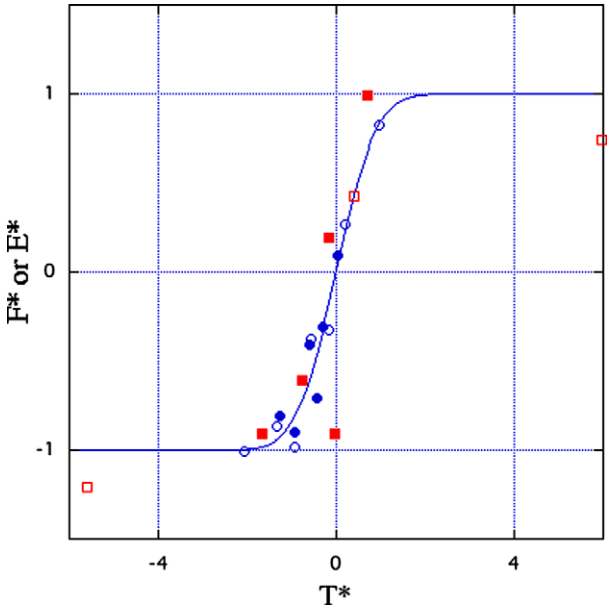

Fig. 4. Reduced absorbed impact energy, E^* (open symbols) and ductile fraction, F^* (bulk symbols) as a function of the reduced temperature, T^*, from CVN samples in steel F82H [13]. Master curve (full line, Eq. (6)), circles and squares correspond to specimens respectively machined along the perpendicular or the parallel to the rolling direction [13].

Table 3
Model parameters, s and T_0, extracted from experimental values of the ductile fraction in steel F82H. T_{DBT} is the transition temperature value reported in [13].

Estimated through $R_d = (E(T) - E_{LS})/(E_{US} - E_{LS})$ (see text)		From experimental ductile fraction data		T_{DBT} (K)	Reference
T_0 (K)	σ (K)	T_0 (K)	σ (K)		
228	18.5	232	22	234	[13][a]
218	.6	229	24	225	[13][b]

[a] Impact direction: normal.
[b] Impact direction: parallel to the rolling direction.

underlying the ductile-to-brittle transition are fundamentally similar. Moreover, this behavior suggests that the model successfully incorporates the dispersion of the microstructure present in the experimental samples.

It is well known that the values of the transition temperature and of the lower and upper shelf energies depend crucially on the size of samples [12]. It is therefore interesting to seek the existence of the master curve for data collected using samples of different sizes such as CVN, miniature CVN (MCVN) and disks adapted to small punch (SP) tests. Fig. 3 displays the master curve and data from CVN, MCVN and SP samples for the steel F82H (Table 2). Again, all the data align on the master curve further supporting the conclusions drawn above from Figs. 1 and 2.

Eq. (4) expresses the absorbed energy during an impact test as an ideal mixture of plastic energies related to regions of the tested sample failing in the brittle, mixed or ductile modes. An easy estimation of the ductile fraction, $f(T)$, is given by the ratio, $R_d = (E(T) - E_{LS})/(E_{US} - E_{LS})$ though this fraction can also be directly determined by examining quantitatively the fracture surfaces. Fig. 4 displays the master curve, $E^*(T^*)$, together with absorbed energy and ductile fraction data for steel F82H [13]. The model fits satisfactorily the experimental data proving thereby that Eq. (4) provides a reasonable description of the amount of absorbed plastic energy as a function of the temperature. The experimental data in Fig. 4 were collected by Shiba et al. [13] who used two types of rolled samples so as to align the rolling direction parallel or normal to the impact direction. These authors report that the corresponding transition temperatures are different by, $\delta T = 9$ K (Table 3). However, by using their ductile fraction data, T_0 values obtained in the present work for the two series of samples are in closer agreement, $T_{//} = 229$ K and $T_{\perp} = 232$ K, with similar dispersion parameters, σ, suggesting the ductile fraction be less affected by experimental errors than the absorbed energy.

In Tables 1 and 2, values of the mean squared deviation, σ, are also reported for each of the data sets used for testing the statistical model. These are reasonably small, as they do not exceed in general 3% of the melting temperature. In absence of more extended experimental data from samples with different microstructures, the sensitivity of this parameter to the dispersion of particular micro-structural features cannot be assessed. However, it is remarkable that before and after irradiation [8], this parameter does not change significantly (Table 1).

4. Discussion

The statistical model proposed in this work, describes the ductile-to-brittle transition at the macroscopic level at which the dispersion of micro-structural features superimposes the aspects revealed by the microscopic vision of this phenomenon [1–3]. Its principal advantage is to reveal the universal features of the transition by means of the master curve obtained by rescaling the coordinates, absorbed energy or ductile fraction and temperature. Experimental data for any material, type of test (Charpy or small punch) and condition (as prepared or after irradiation) align on the master curve after coordinate-rescaling, specified by the best fit values of E_{LS}, E_{US}, σ and T_0. The standard deviation, σ, is directly related to the micro-structural dispersion and offers a rational mean to test its influence on the transition. To this end, absorbed energy and ductile fraction from quantitative fractography are both needed as a function of the temperature, which are not always available so that progress in the matter may imply resorting to new experiments.

Different macroscopic definitions of the ductile-to-brittle transition temperature from Charpy tests can be found in the literature, which correspond to an arbitrarily defined amount of absorbed plastic energy, expressed as a fraction of the upper shelf energy (USE). On the opposite, within the statistical model, $T_{DBT} = T_0$, is uniquely defined by the condition, $d^2E_{absorbed}/dT^2 = 0$, that is by the temperature at the inflexion point of the graph, $E = E(T)$ (Eq. (4)). If any physical meaning could be assigned to T_{DBT}, we speculate that this would be possible only at, $T_{DBT} = T_0$, the single remarkable point on this curve [16].

Finally, T_0 can be equally determined from the absorbed energy or the ductile fraction changes as a function of the temperature. However, the two methods are not equivalent since the latter involves only two adjustable parameters, σ and T_0. Therefore, experimental errors contribute differently to the values of the adjustable parameters of the statistical model depending on the method employed. It is likely that ductile fraction data are affected to a lesser extent by uncertainties than are absorbed plastic energy values. More systematic work is needed to clarify this specific point. Another unconditional advantage of the quantitative fractography is that assessing the influence of percolation of brittle (ductile) regions on the macroscopic failure of materials is straightforward. Thus this approach is likely to reveal in the future key features of the transition and possibly trigger better understanding of the underlying mechanisms.

5. Conclusion

In this work, the influence of the micro-structural dispersion on the ductile-to-brittle transition of fracture is modeled via a statistical approach. The model proposed has universal features expressed by a master curve on which align renormalized experimental data of absorbed energy or ductile fraction as a function of the temperature, irrespective of the considered material, specimen sizes and micro-structural conditions. The effectiveness of this statistical model has been tested by confrontation to experimental data for steels and refractory metals taken from the literature.

Acknowledgements

Constant support and encouragements by D. Mazière are warmly acknowledged. One of us (V. Pontikis) thanks J. Henry and F. Tavassoli for help and useful discussions.

References

[1] D. François, A. Pineau (Eds.), From Charpy to Present Impact Testing, Elsevier Science Ltd., and ESIS, 2002.
[2] A.S. Argon, J. Eng. Mater. Technol. 123 (2001) 1.
[3] G.T. Hahn, Metall. Trans. A 15 (1984) 947.

[4] R. Moskovic, P.L. Windle, A.F. Smith, Metall. Mater. Trans. A 28 (1997) 1181.
[5] P. Hausild, I. Nedbal, C. Berdin, C. Prioul, Mater. Sci. Eng., A 335 (2002) 164.
[6] M.T. Todinov, Mater. Sci. Eng., A 265 (1999) 1.
[7] M.T. Todinov, M. Novonic, P. Bowen, J.F. Knott, Mater. Sci. Eng., A 287 (2000) 116.
[8] P. Soulat, B. Houssin, P. Bocquet, M. Bethmont, CEA, Technical Report NT-SRMA 90-1857 (1990); M.H. Mathon, Ph.D. Thesis No. 3619, Orsay University, Report No. CEA-R-5701 (1995).
[9] D. Padhii, J.J. Lewandowski, Metall. Mater. Trans. A 34 (2003) 967.
[10] M.L. Grossbeck, R.W. Odom, CRADA Final Report, ORNL 96-0432, ORNL M 6554 (1998).
[11] M. Rieth, B. Dafferner, J. Nucl. Mater. 342 (2005) 20.
[12] J. Kameda, X. Mao, J. Mater. Sci. 27 (1992) 983.
[13] K. Shiba, N. Yamanouchi, A. Tohyama, Fusion Materials Semi-Annual Progress Reports, vol. 20, 1996, p. 190.
[14] X. Jia, Y. Dai, J. Nucl. Mater. 323 (2003) 360.
[15] G.E. Lucas, G.R. Odette, J.W. Sheckherd, K. Edsinger, B. Wirth, Fusion Materials Semi-Annual Progress Reports, vol. 20, 1996, p. 147.
[16] R.L. Klueh, D.S. Gelles, S. Jitsukawa, A. Kimura, G.R. Odette, B. van der Schaaf, M. Victoria, J. Nucl. Mater. 307–311 (2002) 455.
[17] L.E. Schubert, M.L. Hamilton, D.S. Gelles, Fusion Materials Semi-Annual Progress Reports, vol. 21, 1996, p. 151.